



On the role of clouds in the fair weather part of the global electric circuit

A. J. G. Baumgaertner¹, G. M. Lucas¹, J. P. Thayer¹, and S. A. Mallios²

¹Department of Aerospace Engineering Sciences, University of Colorado Boulder, Boulder, Colorado, USA

²Communications and Space Sciences Laboratory, Department of Electrical Engineering, Penn State University, University Park, Pennsylvania, USA

Correspondence to: A. J. G. Baumgaertner (work@andreas-baumgaertner.net)

Received: 20 March 2014 – Published in Atmos. Chem. Phys. Discuss.: 15 April 2014

Revised: 11 July 2014 – Accepted: 18 July 2014 – Published: 25 August 2014

Abstract. Clouds in the fair weather return path of the global electric circuit (GEC) reduce conductivity because of the limited mobility of charge due to attachment to cloud water droplets, effectively leading to a loss of ions. A high-resolution GEC model, which numerically solves the current continuity equation in combination with Ohm's law, is used to show that return currents partially flow around clouds, with current divergence above the cloud and convergence below the cloud. An analysis of this effect is presented for various types of clouds, i.e., for different altitude extents and for different horizontal dimensions, finding that the effect is most pronounced for high clouds with a diameter below 100 km. Based on these results, a method to calculate column and global resistance is developed that can account for all cloud sizes and altitudes. The CESM1(WACCM) (Community Earth System Model – Whole Atmosphere Community Climate Model) as well as ISCCP (International Satellite Cloud Climatology Project) cloud data are used to calculate the effect of this phenomenon on global resistance. From CESM1(WACCM), it is found that when including clouds in the estimate of resistance the global resistance increases by up to 73 %, depending on the parameters used. Using ISCCP cloud cover leads to an even larger increase, which is likely to be overestimated because of time averaging of cloud cover. Neglecting current divergence/convergence around small clouds overestimates global resistance by up to 20 % whereas the method introduced by previous studies underestimates global resistance by up to 40 %. For global GEC models, a conductivity parameterization is developed to account for the current divergence/convergence phenomenon around clouds. Conductiv-

ity simulations from CESM1(WACCM) using this parameterization are presented.

1 Introduction

The global electric circuit (GEC) is a system of currents spanning from the troposphere to the ionosphere. Currents totaling 1–2 kA, are generated by thunderstorms, which charge the ionosphere to approximately 250 kV, and return to the Earth's surface in fair weather and semi-fair weather regions with a current density of approximately 2 pA m⁻². The atmosphere acts as a resistor with a global resistance of approximately 150–300 Ω. For summaries on atmospheric electricity and the GEC see, e.g., Rycroft et al. (2008) and references therein.

Atmospheric electrical conductivity (the inverse of resistivity) largely determines the fair weather current distribution and global resistance. Conductivity, σ , is proportional to the product of ion mobilities, μ^+ , μ^- , and ion concentration, n :

$$\sigma = ne(\mu^+ + \mu^-), \quad (1)$$

where e is the elementary charge. Ion concentration for positive and negative ions is assumed to be equal and is determined by the equilibrium of ion production and loss rate. Ion production in the lowermost troposphere is mostly due to radioactive decay from radon emitted from the ground, whereas cosmic rays are the main ionization source in the upper troposphere and stratosphere. Ion–ion recombination and ion attachment to aerosols and cloud droplets lead to a loss of ions for conductivity. Detailed descriptions of conductivity

are provided by Baumgaertner et al. (2013), B13 hereafter; Tinsley and Zhou (2006), TZ06 hereafter; Rycroft et al. (2008); and Zhou and Tinsley (2010), ZT10 hereafter.

Our purpose here is to characterize the role of clouds in the fair weather part of the GEC, hereby defined as clouds that do not contribute to the source current of the GEC and are located in the GEC's current return path. We will characterize these types of clouds by studying the current flow, potentials, and resistances in the local environment of these clouds. Only a small number of authors have studied these clouds so far. ZT10 were the first to include and parameterize these clouds in global calculations of conductivity and resistance. They suggested a reduction of conductivity between 1 and 2 orders of magnitude inside the cloud. Their technique is further discussed in Sect. 5. Nicoll and Harrison (2009) presented air-to-earth current density measurements from two sites in the UK, together with solar radiation measurements, and showed that current density below the cloud can be reduced, depending on cloud height and cloud thickness. Space charge development at the boundaries of clouds in the fair weather part of the GEC has been addressed by Zhou and Tinsley (2007), using model simulations, whereas a discussion of measurements of cloud edge charging from balloon flights has been presented by Nicoll and Harrison (2010). Zhou and Tinsley (2012) discuss time dependent charging of the cloud edges. A feedback of cloud edge charging on cloud evolution is discussed by Harrison and Ambaum (2009). Note that many of the studies above aimed at discussing cloud electricity in the context of speculated relevance for weather and climate.

Cloud water droplets absorb ions, both through diffusion and conduction (Pruppacher and Klett, 1997, chapter 18.3.1). The effects of weakly electrified clouds can be described based on their ice and liquid droplet number concentrations and radii. Inside clouds, ion number concentration n is constrained by the equation

$$\frac{dn}{dt} = q - \alpha n^2 - n \sum_{i,r} \beta(r_i) S(i, r) - 4\pi D n \sum_r N_r A_r. \quad (2)$$

The first term on the right hand side refers to the ion pair production per unit volume, where q is the ionization rate. The second term corresponds to the ion-ion recombination, where α is the ion-ion recombination rate coefficient. The third term describes the ion attachment to neutral aerosol particles, where $\beta(r_i)$ is the attachment rate coefficient to neutral aerosol particles of type i , with radius r_i and concentration S . Finally, the last term refers to the ion attachment to cloud particles through diffusion, where N_r is the cloud droplet concentration, A_r the droplet radius, and D is ion diffusivity given by

$$D = \frac{\mu k T}{e}. \quad (3)$$

As discussed by Pruppacher and Klett (1997), for fair weather conditions the electric fields are small such that conduction can be neglected.

For the static case considered here, Eq. (2) becomes quadratic in n . Note that Eq. (2) describes the ion attachment to cloud droplets as a loss of ions because the mobility of the ionized droplets is very small such that they are effectively lost for electrical conductivity.

From conductivity, column resistance and global resistance can be derived, which are both important parameters for the GEC. Note, however, that the concept of column resistance is based on the assumption of small horizontal gradients in potential and conductivity, i.e., only vertically flowing currents. Strong horizontal gradients in potential and conductivity violate this approach, as will be demonstrated in the next section.

Column resistance is defined as the vertical integration of the reciprocal of conductivity:

$$R_{\text{col}} = \int_{\text{surface}}^{\text{ionosphere}} \frac{1}{\sigma(z)} dz, \quad (4)$$

where dz are the layer thicknesses. Then global resistance can be calculated as the horizontal integral of reciprocal column resistance:

$$R_{\text{tot}}^{\text{col}} = \left(\iint \frac{r^2 \cos(\lambda) d\phi d\lambda}{R_{\text{col}}(\phi, \lambda)} \right)^{-1}, \quad (5)$$

where r is the Earth's radius, ϕ is longitude, and λ is latitude.

Global models of conductivity generally do not resolve clouds. To account for a model grid cell cloud cover fraction f and a reduction of conductivity by a factor η inside a cloud, ZT10 and B13 used the law of combining resistors in parallel and derived

$$\sigma'(z) = (1 - f(z))\sigma(z) + \eta f(z)\sigma(z) \quad (6)$$

to correct for cloud reduction of conductivity. However, the parallel resistor law can only be applied if the resistors are connected, i.e., the same potential must be present at the connection points. For a cloud that would mean that there is equal potential above the cloud cover fraction of the grid box and above the clear-air fraction of the grid box at the same height, i.e., no horizontal potential gradient in each grid box. Analogously, no horizontal potential gradient would be allowed at the level below the cloud. With this approach it would follow that most of the current flows around the cloud because of the large resistance of the cloud. This is depicted in Fig. 1a, showing the current flow (arrows) and average column resistance R_{col} . In Sect. 3, using a GEC model, it will be shown that only for very small clouds can the horizontal resistance above/below the cloud be neglected, allowing one to assume uniform horizontal potential. The approach here is therefore termed the small cloud approximation. Note that

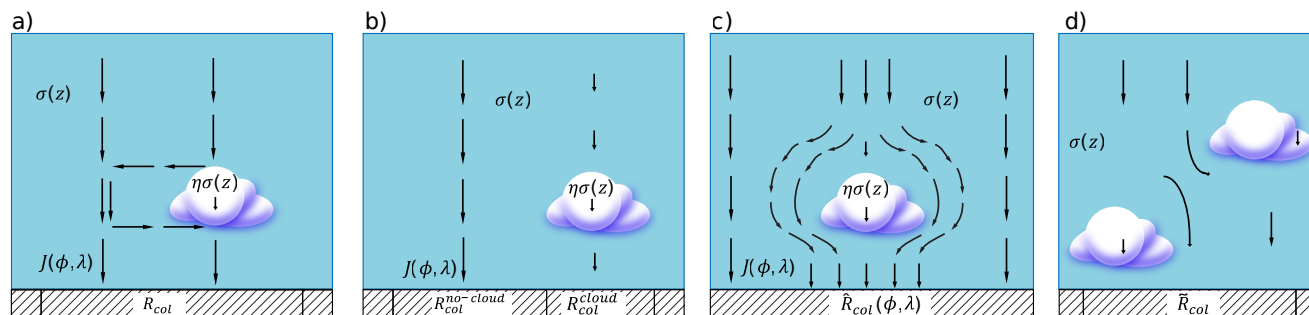


Figure 1. Schematics of cloud modifications of conductivity and column resistance. Arrows denote current direction and the current density magnitude in a qualitative sense. Single cloud, with current mainly flowing around the cloud as assumed in the small cloud approximation (a). Single cloud, only allowing for vertical currents as assumed in the large cloud approximation (b). Current divergence/convergence around the cloud, and “effective column resistance” as a function of latitude and longitude, employed for the current continuity approach (c). Model grid column with cloud fraction and current continuity approach column resistance \tilde{R}_{col} (d).

ZT10 and B13 did not consider the potential changes and assumed their approximation was valid for all cloud sizes.

A different approach to account for clouds, here termed the large cloud approximation, uses the fact that the ionosphere as well as the Earth’s surface both have equal potential on a scale of up to the order of magnitude of 1000 km, thus on a scale applicable for cloud resistance calculations. Resistance of a column with partial cloud cover f is then estimated using the parallel resistor law:

$$\frac{1}{R_{col}} = \frac{f}{R_{col}^{cloud}} + \frac{1-f}{R_{col}^{no-cloud}}, \quad (7)$$

where R_{col}^{cloud} is calculated with Eq. (4) using a conductivity profile with conductivity $\eta\sigma(z)$ for levels z with cloud cover, i.e., assuming 100 % cloud cover in the grid cell. The assumed current flow and the column resistances $R_{col}^{no-cloud}$ and R_{col}^{cloud} are depicted in the schematic of Fig. 1b. The approach can be extended to account for several layers of clouds. However, this formulation only applies when the currents are assumed to flow vertically (normal to Earth’s surface). For small clouds, where currents flow around the cloud as will be shown in Sect. 3, horizontal currents arise above and below the cloud, and the approximation of Eq. (7) only holds for large clouds. For a general solution, integration would need to occur over lines of constant potential. A demonstration of the error resulting from a simple example problem can be seen in Romano and Price (1996).

To account for small-scale conductivity changes through clouds, global resistance cannot be calculated with integrals over conductivity and must be derived from Ohm’s law by calculating the current flowing over a boundary with a fixed potential,

$$R_{tot}^{Ohm} = \frac{\Phi_I}{I_{tot}}, \quad (8)$$

where Φ_I is the ionospheric potential and I_{tot} the total GEC current, which can be calculated as the surface integral of the

downward component of the air-to-earth current densities:

$$I_{tot} = \iint J_{\downarrow air-to-earth}(\phi, \lambda) r^2 \cos(\lambda) d\phi d\lambda. \quad (9)$$

Ionospheric potential, Φ_I , and current density, J , can only be calculated by solving the current continuity equation for the GEC. Then clouds of all sizes are completely accounted for in the estimate of global resistance. However, global 3-D models of the GEC are generally not employed on spatial resolutions that resolve clouds, similar to conductivity models or climate models. Therefore, an approach is presented here that is based on replacing column resistance by an “effective column resistance” \hat{R}_{col} , which can truly account for any type of clouds in the column, yielding the true global resistance R_{tot}^{Ohm} by integrating over \hat{R}_{col} as in Eq. (5). This new approach is termed the current continuity approach as the current continuity equation in combination with Ohm’s law is solved to derive the current distribution in the vicinity of the cloud using a local area, high-resolution model that can resolve the considered clouds.

We define \hat{R}_{col} as

$$\hat{R}_{col}(\phi, \lambda) = \frac{\Phi_I}{J_{\downarrow air-to-earth}(\phi, \lambda)} \quad (10)$$

because then, making use of the definitions in Eqs. (5), (8) and (9),

$$R_{tot}^{col} = \left(\iint \frac{r^2 \cos(\lambda) d\phi d\lambda}{\hat{R}_{col}(\phi, \lambda)} \right)^{-1}, \quad (11)$$

$$= \Phi_I \cdot \left(\iint J_{\downarrow air-to-earth}(\phi, \lambda) \cdot r^2 \cos(\lambda) d\phi d\lambda \right)^{-1}, \quad (12)$$

$$= \frac{\Phi_I}{I_{tot}} = R_{tot}^{Ohm}. \quad (13)$$

With this new definition, horizontal integration of the reciprocal effective column resistance yields the global resistance R_{tot}^{Ohm} for any type of circuit between the ground and

the ionosphere, and will be used to derive the net effect of clouds on the (semi-)fair weather part of the GEC. For the current continuity approach, Fig. 1c depicts a schematic of the current flow around the cloud, here termed the divergence/convergence phenomenon, and the effective column resistance \widehat{R}_{col} , which is a function of latitude and longitude.

For the discussion of global resistance, it is also important to note that for deriving time-averaged global resistance $\overline{R}_{\text{tot}}$, time averaging has to be performed over global resistance, $R_{\text{tot}}(t)$, and not over conductivity or column resistance. This is due to the fact that parallel column resistances are averaged according to the parallel resistor law to derive global resistance. For example, first averaging cloud fractions $f(t)$ over time to derive \overline{f} and then using \overline{f} to calculate conductivity, column resistance, and global resistance leads to an overestimation of global resistance. This will be discussed further in the discussion below.

Section 2 describes the conductivity module and a GEC model that are used to quantify the effects on currents and potentials. In Sect. 3, high-resolution GEC simulations of individual clouds in the fair weather region are presented. The effect of these findings on a global scale is discussed in Sect. 4. Section 5 develops and evaluates a parametrization of clouds in the fair weather region of the GEC for use in conductivity models.

2 Model and data set descriptions

2.1 GEC model

The defining equations for current flow are the current continuity equation and Ohm's law (see, e.g., Zangwill, 2013, chapter 9.4):

$$\nabla \cdot J = S, \quad (14)$$

$$J = \sigma E, \quad (15)$$

where J is the current density, S is the negative time derivative of charge density, which describes thunderstorms and electrified clouds, σ is conductivity, and E is the electric field. If no changing magnetic fields are present, the electric field is defined as the gradient of a potential Φ : $E = -\nabla\Phi$, in which case Ohm's law can be written as

$$J = -\sigma \nabla \Phi. \quad (16)$$

Combining Ohm's law and the current continuity equation yields the partial differential equation (PDE):

$$-\nabla \cdot [\sigma \nabla \Phi] = S. \quad (17)$$

To solve this for the current density and potential distributions, we employ a finite element model formulation, which requires a variational formulation of the PDE. Incorporating

boundary conditions, the problem can be written as

$$\begin{aligned} -\nabla \cdot [\sigma \nabla \Phi] &= S \quad \text{in } \Omega, \\ \Phi &= \Phi_E \quad \text{on } \Gamma_E, \\ \sigma \nabla \Phi \cdot n &= 0 \quad \text{on } \Gamma_L \text{ and } \Gamma_R, \end{aligned} \quad (18)$$

where Ω represents the domain that the PDE is solved for (i.e., a region of the atmosphere), Γ_E is the earth boundary, and a Dirichlet boundary condition is implemented with Φ_E , the fixed potential of the earth, here arbitrarily taken to be zero. Γ_L and Γ_R represent the left and right boundaries of the domain where the current is expected to be vertical far away from any clouds. For the top boundary to the ionosphere, Γ_I , a Neumann boundary condition can be chosen:

$$\nabla \Phi \cdot n = 0 \quad \text{on } \Gamma_I. \quad (19)$$

Alternatively, it is possible to use a Dirichlet boundary condition (i.e., enforce a fixed value at the top):

$$\Phi = \Phi_I \quad \text{on } \Gamma_I. \quad (20)$$

The solution is obtained over the domain Ω where σ varies exponentially in height, and within Ω_C (the cloud) $\sigma_c = \eta\sigma$, where η is a constant.

The variational form of the PDE solves for $\Phi \in V$, where V is a suitable function space, such that

$$a(\Phi, v) = L(v) \quad \forall v \in V, \quad (21)$$

and

$$\begin{aligned} a(\Phi, v) &= \int_{\Omega \setminus \Omega_C} \sigma \nabla \Phi \cdot \nabla v dx + \int_{\Omega_C} \sigma_c \nabla \Phi \cdot \nabla v dx \\ L(v) &= \int_{\Omega} S v dx, \end{aligned} \quad (22)$$

where integrals over the Γ_L and Γ_R boundaries would appear in $L(v)$ if they were non-zero.

This formulation was implemented in the FEnics Python program (Logg et al., 2012) to obtain the potential and current distribution throughout the domain.

With the current densities known throughout the domain, one can integrate over the lower boundary to determine the total current

$$I_{\text{tot}} = \int_{\Gamma_E} -\sigma \nabla \Phi ds. \quad (23)$$

Then one can determine the global resistance following Eq. (8).

For the GEC cloud simulations presented in the next section, we specify a fixed potential equal to 300 kV at 60 km altitude and assume sources of charge to be unchanging with time.

The GEC model has a flexible horizontal and vertical resolution. For the following section, the resolution and domain size were adjusted to suit the studied cloud size such that the cloud and the region below the cloud are resolved. For example, for a cloud with 10 km diameter, a horizontal resolution of 1 km, a vertical resolution of 100 m, and a domain diameter of 50 km are sufficient. For the upper boundary, a height of 60 km is used for all simulations.

2.2 Conductivity model

Conductivity calculations are performed using the Whole Atmosphere Community Climate Model (WACCM) (Marsh et al., 2013) which is part of the CESM1 (Community Earth System Model), with an additional module to calculate conductivity. The driving parameters in the conductivity module are temperature, density, pressure, aerosol concentrations (from CESM1(WACCM) simulations with CARMA (Community Aerosol and Radiation Model for Atmospheres)), and optionally cloud coverage. The model is described and evaluated in detail within B13, using average atmospheric and solar conditions. Here, we use the Specified Dynamics version of WACCM (SD-WACCM), where temperatures and winds are nudged to meteorological assimilation analysis results (GEOS5) (see Lamarque et al. (2012) for a description).

Note that the vertical coordinate system of CESM1(WACCM) is mostly based on atmospheric pressure, which is very adequate for conductivity and column resistance calculations because of the exponential increase in conductivity. The level spacing is approximately 300 m near the surface and increases to several kilometers in the stratosphere, although this depends on the chosen vertical resolution. The horizontal resolution of CESM1(WACCM) is also very flexible, and can range from 25 km to 500 km in latitude and longitude, depending on the chosen simulation grid. The simulations presented below use a grid with 1.9° resolution in latitude and 2.5° in longitude.

2.3 ISCCP data set

The ISCCP (International Satellite Cloud Climatology Project) uses data from a suite of weather satellites. Documentation and further references are provided by Rossow and Schiffer (1999). We use the ISCCP cloud-type classification and the associated mean annual cloud coverage data, which is derived from daytime measurements. ISCCP classifies clouds in three altitude regimes (up to 680 hPa, between 440 and 680 hPa, and above 40 hPa), and further into cumulus, stratocumulus, stratus (low clouds), altocumulus, altostratus, nimbostratus (middle clouds), and cirrus, cirrostratus, deep convection (high clouds).

Unfortunately, ISCCP does not provide global cloud thickness data. Cumulus/stratocumulus and stratus clouds were chosen to span the 1–2 km height, altostratus to span 3–5 km, altocumulus to span 2–3 km, nimbostratus to span 2–5 km,

and cirrus/cirrostratus to span 8–9.5 km. Deep convective clouds are not considered, as they are generally electrified. Other cloud categories, especially nimbostratus, might also experience electrification, but since there is not enough consistent understanding of electrified non-thunderstorm clouds (MacGorman and Rust, 1998), they will be considered to be in the semi-fair weather region in the global resistance estimates below. However, further work appears necessary for a better classification of cloud electrification. This will be discussed further in Sect. 5.

3 Single clouds

For the GEC simulations, an average background (cloud-free) conductivity profile from the work by B13 is used with no horizontal variability. The domain borders in the horizontal were chosen to be sufficiently far away from the cloud edge, so the domain size increases for simulations with larger horizontal cloud sizes. To simulate the effect of a single cloud, conductivity is reduced inside the cloud. As previously shown by Zhou and Tinsley (2010), the conductivity reduction inside a cloud can be approximated by a fraction η of ambient conductivity. Estimates for η range from 1/10 (Nicoll and Harrison, 2009) to 1/50 (Zhou and Tinsley, 2010).

Figures 2 and 3 present (a) the current density distribution, (b) air-to-earth current densities, (c) column resistances, and (d) potential differences for a simulation of a cirrus cloud (Fig. 2) and a stratus cloud (Fig. 3). For both cases a cloud diameter of 10 km was chosen, and $\eta = 1/50$.

For the cirrus cloud a thickness of 1.5 km, spanning from 8 to 9.5 km was chosen. The top panel in Fig. 2 depicts the current density streamlines (tangent to the current vector). As expected, there is a strong reduction from an average current density of 2.5 pA m^{-2} to 0.6 pA m^{-2} inside the cloud. However, the streamlines show that currents bend around the cloud, leading to higher-than-average currents (red) at the edges. There is a current divergence above the cloud, and convergence below. The effect on the air-to-earth current density is shown in Fig. 2b. The red line depicts the air-to-earth current densities if only vertical currents were permitted, i.e., the ionospheric potential divided by the column resistance R_{col} . The blue line shows the model result, indicating that the current density reduction is in fact less severe but spread out several kilometers past the cloud edge.

In Fig. 2c, showing column resistance, the red line depicts the vertically integrated column resistance R_{col} , and the blue line depicts the column resistance \hat{R}_{col} calculated as ionospheric potential divided by simulated air-to-earth current density, as defined in Eq. (10) (see also the schematic in Fig. 1).

Figure 2d depicts the potential distribution around the cloud. Clearly, even for the 10 km cloud shown here, there is a strong horizontal potential gradient both above (at 9.5 km)

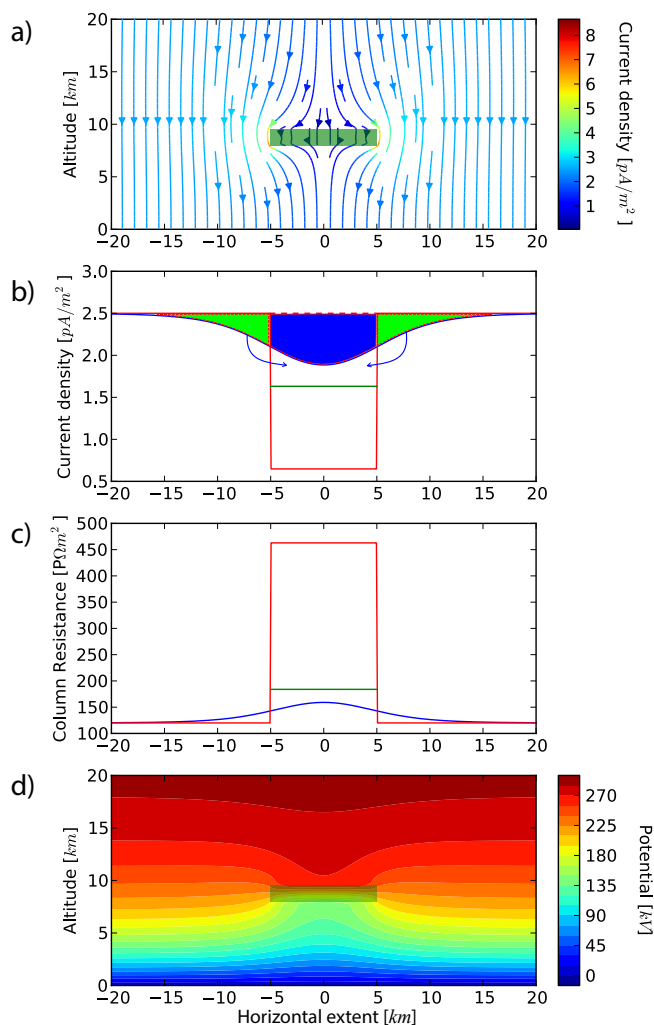


Figure 2. Current streamlines and total current density around a cirrus cloud (indicated by the green box) with a diameter of 10 km, located between 8 and 9.5 km altitude (a). Model air-to-earth current density (blue), restricted to vertical currents only (red), and mean effective cloud current density (green) (b). Effective column resistance \hat{R}_{col} (blue), column resistance for considering vertical currents only R_{col} (red), and mean effective cloud column resistance $\hat{R}_{\text{col}}^{\text{cloud}}$ (green) (c). Potential difference distribution (d).

and below (at 8 km) the cloud, showing that the assumption of the small cloud approximation of equal potential at equal heights does not hold, as mentioned in the introduction.

In order to simplify further studies of cloud effects on larger horizontal domains, it is desirable to replace \hat{R}_{col} with only one value for the cloud area, where the fair weather column resistance remains unchanged. Therefore, we are looking for a new cloud column resistance value $\hat{R}_{\text{col}}^{\text{cloud}}$, that takes into account the partial current flow around the cloud. Because of the divergence/convergence of currents around the cloud, $R_{\text{col}}^{\text{cloud}}$ (red line) does not give the correct average cloud column resistance.

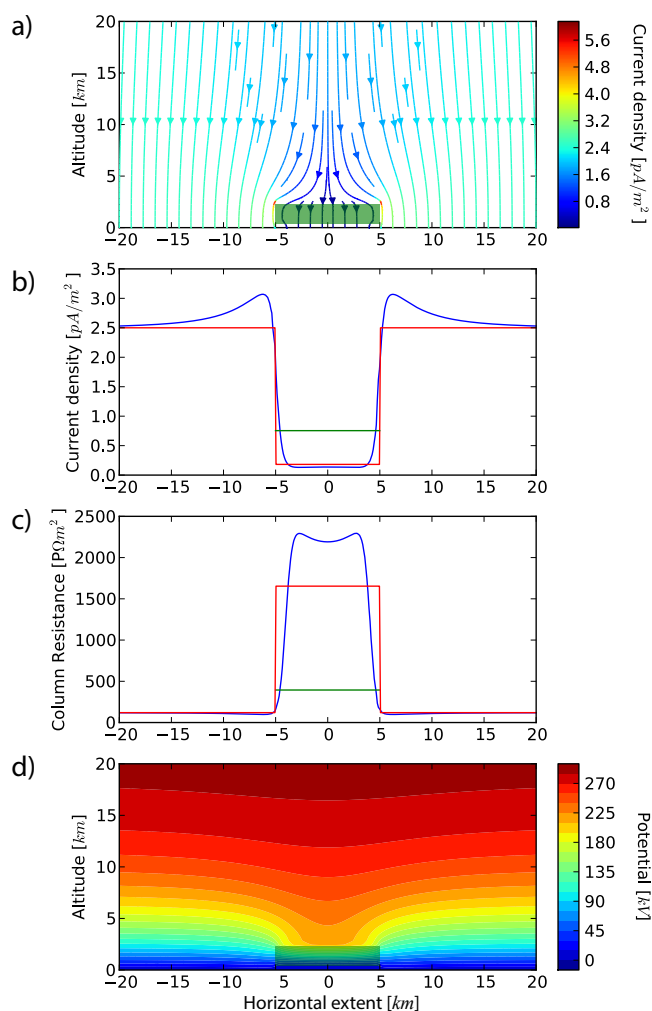


Figure 3. As Fig. 2 but for a stratus cloud between 0.5 and 2.5 km altitude.

It is also possible to formulate this using current density, where the air-to-earth current density is replaced with a fair weather air-to-earth current density, and a semi-fair weather (cloud) air-to-earth current density $\hat{J}_{\text{air-to-earth}}^{\text{cloud}}$, because then

$$\hat{R}_{\text{col}}^{\text{cloud}} = \frac{\Phi_{\text{I}}}{\hat{J}_{\text{air-to-earth}}^{\text{cloud}}} \quad (24)$$

The approach is depicted in Fig. 2b. By integrating $J_{\text{air-to-earth}}^{\text{no-cloud}} - J_{\text{air-to-earth}}$ over the shown domain, i.e., the difference between the blue line and the fair weather current density (green and blue areas), and dividing only by the area of the cloud, the current density reduction is attributed to the cloud area (indicated by arrows). So we define the cloud current density $\hat{J}_{\text{air-to-earth}}^{\text{cloud}}$ as

$$\hat{J}_{\text{air-to-earth}}^{\text{cloud}} = J_{\text{air-to-earth}}^{\text{no-cloud}} - A^{-1} \iint (J_{\text{air-to-earth}}^{\text{no-cloud}} - J_{\text{air-to-earth}}(\phi, \lambda)) d\phi d\lambda, \quad (25)$$

where A is the area of the cloud. The resulting current density is shown as the green line in Fig. 2b.

The green line in panel (c) of Fig. 2 shows the resulting column resistance $\widehat{R}_{\text{col}}^{\text{cloud}}$ using Eq. (24). This is the average column resistance while accounting for the off-vertical currents. Equivalently to $\widehat{J}_{\text{air-to-earth}}^{\text{cloud}}$, $\widehat{R}_{\text{col}}^{\text{cloud}}$ can also be calculated directly. However, horizontal averaging of column resistances requires the use of reciprocal column resistance. Then, $\widehat{R}_{\text{col}}^{\text{cloud}}$ is

$$\widehat{R}_{\text{col}}^{\text{cloud}} = \left(A^{-1} \iint \left(\frac{1}{R_{\text{col}}(\phi, \lambda)} - \frac{1}{R_{\text{col}}^{\text{no-cloud}}} \right) d\phi d\lambda + \frac{1}{R_{\text{col}}^{\text{no-cloud}}} \right)^{-1}, \quad (26)$$

which is mathematically equivalent to the previous definition of $\widehat{R}_{\text{col}}^{\text{cloud}}$. $\widehat{R}_{\text{col}}^{\text{cloud}}$ is also shown in the schematic of Fig. 1c. It is important to note that all derived column resistance values are independent of the ionospheric potential chosen for the simulation.

The results for a stratus cloud with a vertical thickness of 1.5 km and a diameter of 10 km are shown in Fig. 3. Above the cloud, a similar behavior of current spreading towards the cloud edges is found. However, since the cloud is close to the ground, the air-to-earth current density is reduced to a value similar from what would be expected if horizontal currents were neglected, as shown in Fig. 3b. It is interesting to note that this leads to an increase in air-to-earth current density in the cloud-free area next to the cloud edges. Analogously, Fig. 3c shows the column resistances from vertical integration of the reciprocal of conductivity R_{col} (red), the effective column resistance \widehat{R}_{col} (blue), and the average column resistance $\widehat{R}_{\text{col}}^{\text{cloud}}$ (green) as defined above. Similarly to the cirrus cloud, the potential distribution in Fig. 3d depicts large horizontal gradients.

Note that the results are approximately independent of the vertical and horizontal resolution of the simulation as long as the cloud and the region below the cloud are resolved. Only for future studies of cloud edge charges would a higher vertical resolution to resolve the cloud edge and a realistic cloud edge conductivity profile be required.

To compare the current divergence/convergence effect for different cloud types and horizontal dimensions, we compute the ratio $\widehat{R}_{\text{col}}^{\text{cloud}}/R_{\text{col}}^{\text{cloud}}$, shown in Fig. 4, as a function of cloud diameter for a variety of cloud types. Here, cloud types are only distinguished by their altitude regime, using the IS-CCP types. In the future, results from other satellite missions such as the NASA ICESat (Ice, Cloud, and land Elevation Satellite) and CloudSat missions, can be used for more accurate global cloud thickness analysis.

From Fig. 4, one can see the effect is most important for clouds with a diameter of less than 100 km. In the transition range, between 2 and 100 km, generally the effect is more pronounced, i.e., a smaller $\widehat{R}_{\text{col}}^{\text{cloud}}/R_{\text{col}}^{\text{cloud}}$, for

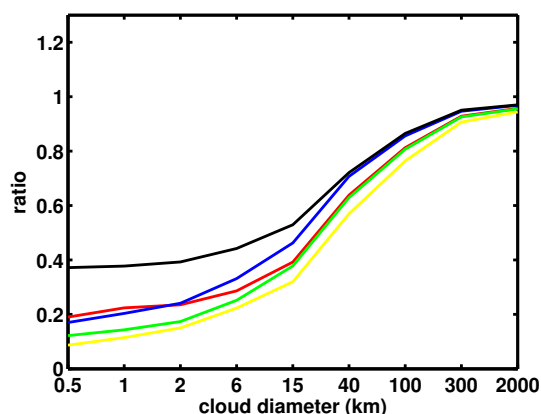


Figure 4. Horizontal-size dependence of $\widehat{R}_{\text{col}}^{\text{cloud}}/R_{\text{col}}^{\text{cloud}}$ for different types of clouds: cumulus and stratocumulus (1–2 km, red), altostratus (3–5 km, green), altocumulus (2–3 km, blue), nimbostratus (2–5 km, yellow), and cirrus (8–9.5 km, black).

clouds with a high cloud bottom for which the current divergence/convergence becomes more important, as seen above. For example, the effect is less pronounced for cumulus and stratocumulus (red) with a bottom height of 1 km than it is for altostratus (green) with a bottom height of 3 km. However, very high clouds such as the cirrus type have a smaller effect on column resistance because of the exponential increase of conductivity with altitude, i.e., changes in conductivity at higher altitudes are less important for column resistance than the same fractional change at lower altitudes. For Fig. 4, this leads to a larger ratio of $\widehat{R}_{\text{col}}^{\text{cloud}}/R_{\text{col}}^{\text{cloud}}$ for cirrus clouds (black).

A sensitivity analysis using $\eta = 1/25$ (not shown) yields increases in the ratio $\widehat{R}_{\text{col}}^{\text{cloud}}/R_{\text{col}}^{\text{cloud}}$ of approximately 0.1 for small clouds, except for cirrus where an increase of approximately 0.2 is found.

4 Global effect

For estimating the impact of clouds in the fair weather part of the GEC on global resistance, it is necessary to take into account the cloud size distribution. Wood and Field (2011) have used MODIS, airplane, and model data to show that the cloud chord length (corresponding to the average cloud diameter, see their paper for more details), x , as well as the projected area obey a power law. For the cloud cover contribution C from clouds larger than x/x_{max} they showed that

$$C(x) = 1 - (x/x_{\text{max}})^{2-\beta}, \quad (27)$$

and found that $\beta \approx 1.7$ and $x_{\text{max}} = 2000$ km. For chord lengths larger than 2000 km, a scale break occurs.

The contribution C_h of any chosen set of cloud horizontal sizes h_i for the intervals $[(h_{i-1} + h_i)/2, (h_{i+1} + h_i)/2]$ can then be calculated.

If we assume this result to be true individually for all types of clouds, the size-dependent cloud cover fraction is then $g(h_i, \text{type}) = f(\text{type}) \cdot C_h(h_i)$, where cloud cover fraction f is given by satellite observations, e.g., by ISCCP, or model simulations.

The high-resolution simulations for single clouds in the previous section are used to derive the ratio $\widehat{R}_{\text{col}}^{\text{cloud}} / R_{\text{col}}^{\text{no-cloud}}$ for every cloud type. Note that the result will be independent of the model source currents or the ionospheric potential.

The values for $R_{\text{col}}(\phi, \lambda)$, from observations or model data, are then used to derive $\widehat{R}_{\text{col}}^{\text{cloud}}$ for every cloud type. The current continuity approach column resistance R_{col} for a cloud cover model or observation column can then be calculated by averaging the individual values for $\widehat{R}_{\text{col}}^{\text{cloud}}(h_i, \text{type})$ weighted by the corresponding cloud cover fraction:

$$\begin{aligned} \widetilde{R}_{\text{col}} = & \left(\sum_{i, \text{type}} \left(\widehat{R}_{\text{col}}^{\text{cloud}}(h_i, \text{type}) \right)^{-1} \cdot g(h_i, \text{type}) \right. \\ & \left. + \left(R_{\text{col}}^{\text{no-cloud}} \right)^{-1} \cdot \left(1 - \sum_{i, \text{type}} g(h_i, \text{type}) \right) \right)^{-1}. \quad (28) \end{aligned}$$

The use of $\widetilde{R}_{\text{col}}$ as column resistance for a column partially covered with clouds is also visualized in Fig. 1d.

Using the ISCCP cloud cover distributions, we estimate the effect on global resistance. Background (cloud-free) conductivity data was obtained from the CESM1(WACCM) simulation used below for annual mean conditions. Table 1 lists global resistance values for a cloud-free atmosphere, the small cloud approximation, the large cloud approximation, the current continuity approach, and total cloud cover averages. Using the small cloud approximation and ISCCP cloud cover data, ZT10 estimated an increase of global resistance through clouds by about 18Ω , similar to the 22Ω here ($\eta = 1/50$).

The large cloud approximation leads to increases of global resistance by up to 188Ω (114 %), whereas with the current continuity approach, taking the current divergence/convergence into account, increases global resistance by 144Ω (87 %). As expected, the latter value lies between the small and large cloud approximations. For $\eta = 1/50$, the small cloud approximation underestimates total resistance by 39 % compared to the current continuity approach, whereas the large cloud approximation overestimates it by 14 %.

Similar to ISCCP, the Earth System Model CESM1(WACCM) was also used to calculate global resistances, using the model cloud cover, which is provided as a function of altitude and horizontal location. There is no information on cloud type in CESM1(WACCM). Therefore, the cloud fractions were grouped to the same three heights as used in ISCCP (see Sect. 2.3). Then the same procedure as for ISCCP can be used to derive column resistances.

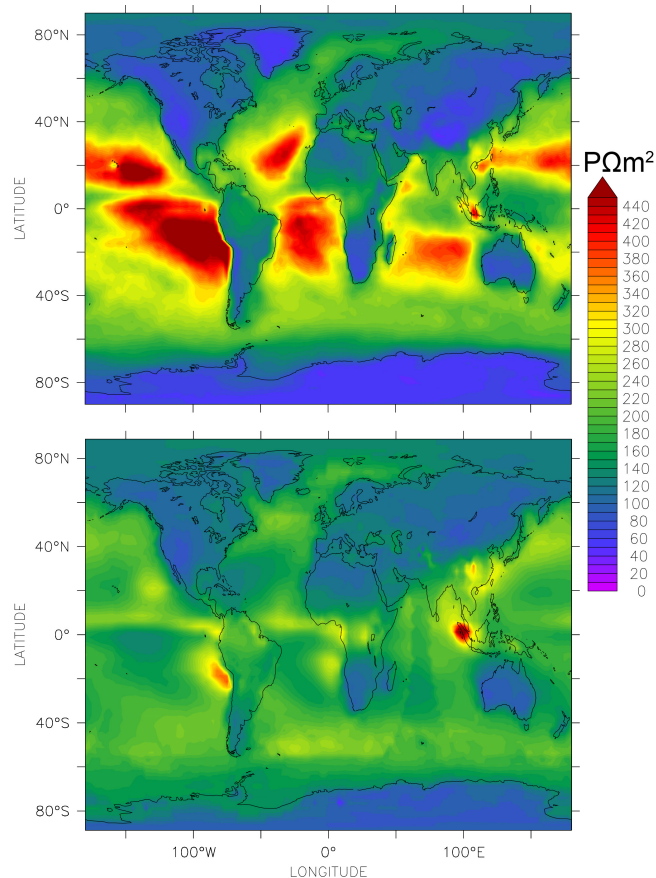


Figure 5. CESM1(WACCM) (top) and ISCCP (bottom) average column resistance ($P\Omega\text{m}^2=10^{15}\Omega\text{m}^2$), taking the current divergence/convergence phenomenon into account ($\eta = 1/50$).

Again, the large cloud approximation overestimates global resistance significantly, by up to 21 %, when compared to the current continuity approach.

Despite the slightly larger total cloud cover, the CESM1(WACCM) global resistances are consistently smaller by up to 37Ω compared to ISCCP for all η . There are several reasons for the discrepancies: first, since the model provides cloud coverage as a function of altitude, there is a major difference in the treatment of cloud thickness compared to ISCCP. Secondly, ISCCP cloud coverage data is only for daytime, which can be significantly different than nighttime coverage. Finally, CESM1(WACCM) uses instantaneous values of cloud cover to calculate conductivity and column resistance, whereas ISCCP only provides time-averaged cloud cover and therefore the derived global resistance is overestimated, as mentioned in the introduction.

The annual mean column resistances, similar to Fig. 7 in B13, are shown in Fig. 5 for ISCCP and CESM1(WACCM). Surprisingly, the model shows areas of higher column resistance in areas of high cloud coverage, yet the global resistance is smaller than from ISCCP, driven by the areas of little cloud coverage, i.e., small column resistance.

Table 1. Annual mean GEC global resistances.

	ISCCP			CESM1(WACCM)		
	$\eta = 1/10$	$\eta = 1/25$	$\eta = 1/50$	$\eta = 1/10$	$\eta = 1/25$	$\eta = 1/50$
Cloud-free atmosphere	165 Ω					
Small cloud approximation	184 Ω	186 Ω	187 Ω			
Large cloud approximation	244 Ω	303 Ω	353 Ω	215 Ω	284 Ω	345 Ω
Current continuity approach	233 Ω	277 Ω	309 Ω	196 Ω	246 Ω	285 Ω
Total cloud cover	66 %			69 %		

The only available measurements of air-to-earth current density depending on cloud coverage were presented by Nicoll and Harrison (2009). The authors found little change in the current density measurements, only fully overcast conditions with thick clouds led to current density reductions. The model simulations support and explain these findings. Unfortunately, the authors did not present their results as a function of cloud size, since such data was not available, so a quantitative comparison or evaluation of the model results is not possible.

5 Parameterization for 3-D conductivity calculations

3-D models used to calculate conductivity generally cannot resolve clouds because of their coarse horizontal resolution and instead operate on cloud cover fractions for each grid box. For the calculation of conductivity in such models, a parametrization is then required to account for the effect of clouds in the fair weather region of the GEC. The 3-D conductivity model results can then be used for global GEC models that solve the relevant PDE to derive global distributions of potentials and currents.

ZT10 have provided a parametrization to account for clouds as discussed in the introduction. However, as shown above, the approximation only holds for very small cirrus clouds and underestimates the resistance increase through clouds significantly.

Here, we introduce a parametrization suitable for all cloud sizes and vertical extents, based on the high-resolution model results of individual clouds presented above. This will yield corrections to conductivity such that the vertical current assumption can be employed again.

In the first step, the current continuity approach column resistance \tilde{R}_{col} is parameterized using the approach to calculate the global effect presented in Sect. 4. The model data required for this are the fair weather column resistance, cloud cover fractions for the pre-defined cloud types for every model grid point, and cloud cover for every model grid point as a function of model layer $f(z)$.

We define effective conductivity $\tilde{\sigma}$ such that

$$\tilde{R}_{\text{col}} = \int \frac{dz}{\tilde{\sigma}(z)}. \quad (29)$$

We assume the following relationship between $\tilde{\sigma}$ and the cloud-free conductivity:

$$\tilde{\sigma}(z) = (1 - f(z))\sigma(z) + \gamma f(z)\sigma(z), \quad (30)$$

where a parameter γ is introduced that will take into account the non-linearity introduced by the current divergence/convergence around the clouds. Note that γ is not an assumed constant as in the work by ZT10, see Eq. (6), but will be derived from the known value for \tilde{R}_{col} for every model column.

Using the assumed form for $\tilde{\sigma}$ from Eq. (30), we can rewrite Eq. (29) as

$$\tilde{R}_{\text{col}} = \sum_{i=1}^n \frac{\Delta z}{\sigma(z)(1 - f(z)(1 - \gamma))} \quad (31)$$

for n model layers with thickness Δz . Equation (31) is a polynomial with degree n for the variable γ . Here, Newton's method is used to numerically approximate γ for the function

$$h(\gamma) = R - \sum_{i=1}^n \frac{\Delta z_i}{\sigma_i(1 - f_i(1 - \gamma))} = 0. \quad (32)$$

The first derivative is

$$h'(\gamma) = \sum_{i=1}^n \frac{\Delta z_i \sigma_i f_i}{(\sigma_i(1 - f_i(1 - \gamma)))^2}. \quad (33)$$

With this, the solution is iteratively approximated using

$$\gamma_{m+1} = \gamma_m - h(\gamma_m)/h'(\gamma_m). \quad (34)$$

While the polynomial in general has n number of solutions, only the largest γ is physically meaningful. For other solutions, conductivity of the layer with the largest cloud cover f becomes negative. The initial guess γ_0 for the largest γ is close to where the fraction reaches singularity,

$$\gamma_0 = 1 - 1/\max(f) + \epsilon. \quad (35)$$

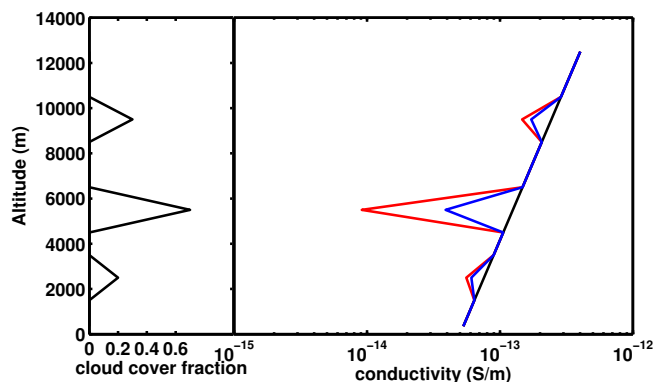


Figure 6. Left: cloud cover fraction of a single column. Right: background (black), ZT10 (blue) and parameterized (red, see text) cloud conductivity profile.

Then Newton's method reliably converges to this solution. With γ from Eq. (30), $\tilde{\sigma}(z)$ can then be calculated.

Figure 6 shows cloud cover (left) and parameterized conductivity (right) profiles for a single column. The parameterized (red) conductivity $\tilde{\sigma}$ is smaller than the background exponential (black) conductivity depending on the cloud cover of that layer. The ZT10 estimate is also shown (blue), where the conductivity reduction is underestimated as discussed above. The corresponding column resistance values are $R_{\text{col}}^{\text{no-clouds}} = 1.0 \times 10^{17} \Omega \text{m}^2$ and $\tilde{R}_{\text{col}} = 2.1 \times 10^{17} \Omega \text{m}^2$. Vertically integrating the conductivity $\tilde{\sigma}$ gives a result numerically identical to \tilde{R}_{col} , as required by the parameterization. Note that the vertical overlap shown here only refers to multiple cloud layers in a grid column but assumes that the individual clouds are not physically overlapping. Such an overlap would lead to mutual coupling of the layers and would need a more advanced treatment which has not been considered here.

The parameterization developed above was implemented as part of the CESM1(WACCM) conductivity module. As above, cloud cover without deep convection was used in order to include only clouds in the (semi-)fair weather region. As an example, the logarithm of parameterized model conductivity for a single longitude and model time is shown in Fig. 7 (top). Local reductions in conductivity correspond to the local cloud cover fraction, which is also shown (black contour lines). The bottom part depicts the column resistance with (black) and without (red) clouds.

As in the previous section, the results also depend on η as well as the assumed cloud thicknesses that are used to derive $\tilde{R}_{\text{col}}^{\text{cloud}} / R_{\text{col}}^{\text{no-cloud}}$ in the high-resolution simulation part.

The effective conductivity distribution, $\tilde{\sigma}$, can be used for global GEC models to calculate potentials and currents, while accounting for sub-grid scale effects of clouds.

Errors from this parameterization will be largest for areas of the globe where certain types or sizes of clouds are different than average distributions. If the cloud thicknesses

are different than the assumed thicknesses, the parameterization will not give accurate results. No global measurements of these parameters are available, so an estimate of the errors made is currently not possible. The parameterization is based on the assumption that these clouds are not electrified. However, if future measurements show that, in addition to deep convective clouds and some nimbostratus or shower clouds, other cloud categories do have electrification, this could significantly alter the global resistance results. The effect of large-scale precipitation on the column resistance is also not taken into account, as such effects are not yet understood.

Further uncertainties in the resistance estimate are due to mutual coupling of clouds if they are close to each other or vertically overlapping. Figure 8 shows current streamlines (top) and column resistance (bottom) around two clouds both with radius 20 km and between 3 and 5 km in the vertical, separated by 3 km in the horizontal. For this simulation, the column resistance in the area between the clouds does not reach the fair weather column resistance, indicating mutual coupling at horizontal distances below approximately 3 km for this cloud type. Note that the coupling is not a superposition, as can be shown from comparisons of the total resistance of the domain, which increases with decreasing distance between clouds. The cloud distance required for mutual coupling varies by cloud type and diameter. Errors of the column resistance parameterization will increase if a significant fraction of small clouds experience mutual coupling. There is currently not enough satellite data available to estimate this global effect.

6 Conclusions

Using high-resolution model simulations of current flow in the return path of the GEC, the role of clouds was investigated. A finite element model was used to solve the relevant PDE, derived from the current continuity equation and Ohm's law, in the vicinity of various cloud sizes and altitudes. Clouds in the GEC current return path, which decrease electrical conductivity, in general, lead to a reduced current density beneath the cloud layer; however, the model shows that currents bend around clouds of limited horizontal extent (< 100 km), with current divergence above the cloud and convergence below. Below the cloud, this leads to larger current densities and effectively a smaller cloud resistivity than expected if only vertical currents were considered. Qualitatively, this agrees with published air-to-earth current density measurements. This phenomenon was found to be important especially for clouds with a diameter below 100 km, and therefore leads to a significant error when using the classical approach to estimate global resistance, i.e., horizontally integrating column resistance. An effective column resistance was introduced which restores the possibility to derive global resistance the classical way. The current continuity approach method is based on the numerical simulations of effective

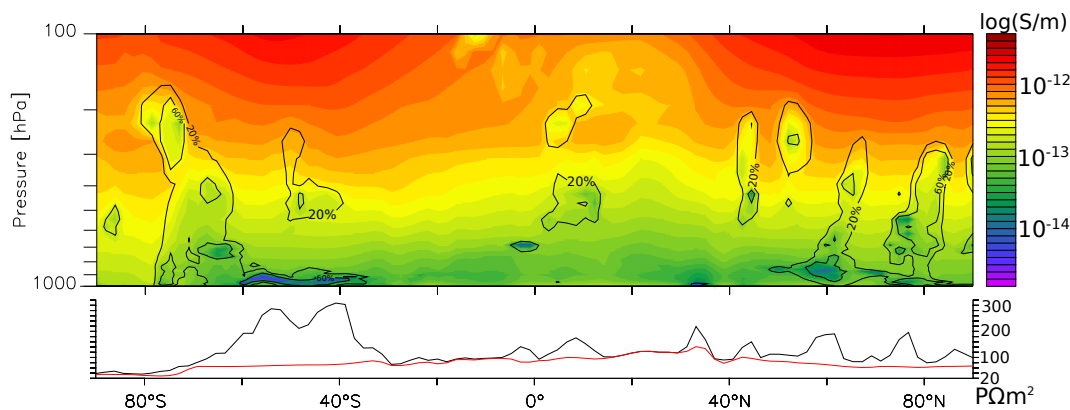


Figure 7. Top: logarithm of conductivity from CESM1(WACCM) for 30° E and 16 September 2005, 00:00 UTC, using the cloud conductivity parameterization. The black contour lines indicate cloud cover fraction (20%, 60%, 100%). Bottom: column resistance for the same location, using the cloud parameterization (black) and neglecting clouds (red).

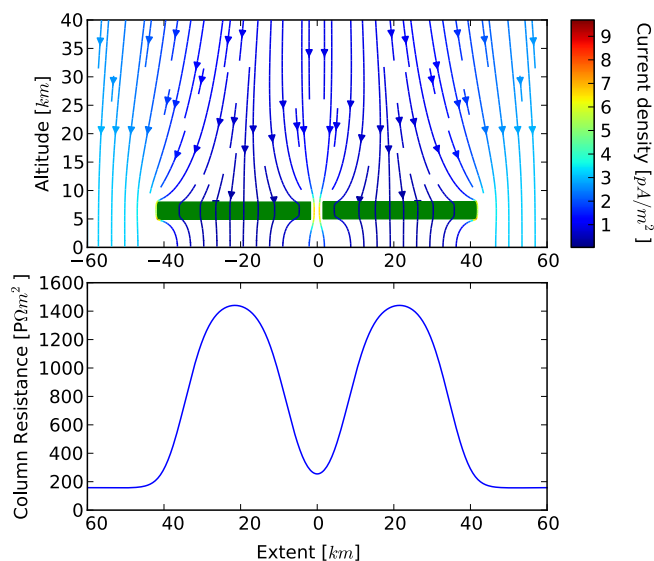


Figure 8. Top: current streamlines in the vicinity of two clouds that are separated by 3 km. Bottom: corresponding column resistance R_{col} .

column resistance for single clouds as a function of cloud size and altitude.

Using the Earth System Model CESM1(WACCM) as well as the ISCCP cloud database, the effect of clouds on global resistance, taking the divergence/convergence phenomenon into account, was estimated. Employing the current continuity approach introduced here, clouds in the fair weather part of the GEC were found to increase global resistance by up to 120 Ω (73 % of the cloud-free atmosphere resistance) in the model, depending on assumed cloud properties. Using ISCCP, increases are even larger but overestimated because of the use of time-averaged cloud cover. A previously published small cloud approximation leads to underestimation of global resistance by up to 40 % whereas a large cloud

approximation, which only considers vertical currents and neglects divergence/convergence, leads to overestimation by up to 20 %. Current divergence/convergence around clouds should therefore not be neglected in studies of the (semi-) fair weather part of the GEC. For this purpose, a parametrization was developed that corrects conductivity depending on model grid cell cloud cover, such that only vertical current flow on the scale of grid columns needs to be considered. However, it is emphasized that for a better quantification of the role of clouds in the GEC, a better understanding of many aspects will be required. This includes improved estimates of the conductivity decrease in clouds, better distinctions between current-generating clouds and other clouds, improved global cloud thickness data, and mutual coupling by vertical overlapping or horizontal proximity. To experimentally validate the presented results, further work will focus on the analysis of vertical electric field measurements from large horizontal arrays of sensors.

Acknowledgements. This work was supported by NSF Award AGS-1135446 to the University of Colorado under the Frontiers in Earth System Dynamics Program (FESD). The National Center for Atmospheric Research is sponsored by the National Science Foundation. We would like to acknowledge high-performance computing support from Yellowstone (Computational and Information Systems Laboratory, 2012). The ISCCP data were obtained from the International Satellite Cloud Climatology Project website <http://isccp.giss.nasa.gov> maintained by the ISCCP research group at the NASA Goddard Institute for Space Studies, New York, NY on 16 January 2014. We have used the Ferret program (<http://www.ferret.noaa.gov>) from NOAA's Pacific Marine Environmental Laboratory for creating some of the graphics in this paper.

Edited by: J. Curtius

References

- Baumgaertner, A. J. G., Thayer, J. P., Neely, R. R., and Lucas, G.: Toward a comprehensive global electric circuit model: Atmospheric conductivity and its variability in CESM1(WACCM) model simulations, *J. Geophys. Res.*, 118, 9221–9232, doi:10.1002/jgrd.50725, 2013.
- Computational and Information Systems Laboratory: Yellowstone: IBM iDataPlex System (NCAR Community Computing), National Center for Atmospheric Research, Boulder, CO, available at: <http://n2t.net/ark:/85065/d7wd3xhc>, 2012.
- Harrison, R. G. and Ambaum, M. H. P.: Observed atmospheric electricity effect on clouds, *Environ. Res. Lett.*, 4, 014003, doi:10.1088/1748-9326/4/1/014003, 2009.
- Lamarque, J.-F., Emmons, L. K., Hess, P. G., Kinnison, D. E., Tilmes, S., Vitt, F., Heald, C. L., Holland, E. A., Lauritzen, P. H., Neu, J., Orlando, J. J., Rasch, P. J., and Tyndall, G. K.: CAM-chem: description and evaluation of interactive atmospheric chemistry in the Community Earth System Model, *Geosci. Model Dev.*, 5, 369–411, doi:10.5194/gmd-5-369-2012, 2012.
- Logg, A., Mardal, K.-A., and Wells, G. N., (Eds.): *Automated Solution of Differential Equations by the Finite Element Method*, Springer Berlin Heidelberg, doi:10.1007/978-3-642-23099-8, 2012.
- MacGorman, D. R. and Rust, W. D.: *The Electrical Nature of Storms*, Oxford University Press, New York, 44–48, 1998.
- Marsh, D. R., Mills, M. J., Kinnison, D. E., Lamarque, J.-F., Calvo, N., and Polvani, L. M.: Climate Change from 1850 to 2005 Simulated in CESM1(WACCM), *J. Climate*, 26, 7372–7391, doi:10.1175/JCLI-D-12-00558.1, 2013.
- Nicoll, K. A. and Harrison, R. G.: Vertical current flow through extensive layer clouds, *J. Atmos. Sol.-Terr. Phys.*, 71, 2040–2046, doi:10.1016/j.jastp.2009.09.011, 2009.
- Nicoll, K. A. and Harrison, R. G.: Experimental determination of layer cloud edge charging from cosmic ray ionisation, *Geophys. Res. Lett.*, 37, L13802, doi:10.1029/2010GL043605, 2010.
- Pruppacher, H. R. and Klett, J. D.: *Microphysics of Clouds and Precipitation*, Kluwer Academic Publishers, Dordrecht, 2nd Edn., 798–799, 1997.
- Romano, J. D. and Price, R. H.: The conical resistor conundrum: a potential solution, *Am. J. Phys.*, 64, 1150–1153, doi:10.1119/1.18335, 1996.
- Rosow, W. B. and Schiffer, R. A.: Advances in Understanding Clouds from ISCCP, *Bulletin of the American Meteorological Society*, 80, 2261–2288, doi:10.1175/1520-0477(1999)080<2261:AIUCFI>2.0.CO;2, 1999.
- Rycroft, M. J., Harrison, R. G., Nicoll, K. A., and Mareev, E. A.: An overview of earth's global electric circuit and atmospheric conductivity, *Space Sci. Rev.*, 137, 83–105, doi:10.1007/s11214-008-9368-6, 2008.
- Tinsley, B. A. and Zhou, L.: Initial results of a global circuit model with variable stratospheric and tropospheric aerosols, *J. Geophys. Res.*, 111, D16205, doi:10.1029/2005JD006988, 2006.
- Wood, R. and Field, P. R.: The distribution of cloud horizontal sizes, *J. Climate*, 24, 4800–4816, doi:10.1175/2011JCLI4056.1, 2011.
- Zangwill, A.: *Modern electrodynamics*, Cambridge University Press, Cambridge, 1st Edn., 276–277, 2013.
- Zarnik, M. S. and Belavic, D.: An Experimental and Numerical Study of the Humidity Effect on the Stability of a Capacitive Ceramic Pressure Sensor, *Radioengineering*, 21, 201–206, 2012.
- Zhou, L. and Tinsley, B. A.: Production of space charge at the boundaries of layer clouds, *J. Geophys. Res.*, 112, D11203, doi:10.1029/2006JD007998, 2007.
- Zhou, L. and Tinsley, B. A.: Global circuit model with clouds, *J. Atmos. Sci.*, 67, 1143–1156, doi:10.1175/2009JAS3208.1, 2010.
- Zhou, L. and Tinsley, B. A.: Time dependent charging of layer clouds in the global electric circuit, *Adv. Space Res.*, 50, 828–842, doi:10.1016/j.asr.2011.12.018, 2012.